

N72-29238

NASA TECHNICAL  
MEMORANDUM



NASA TM X-2613

NASA TM X-2613

CASE FILE  
COPY

LIQUID INFLOW TO INITIALLY EMPTY  
CYLINDRICAL TANKS IN LOW GRAVITY

*by Charles M. Spuckler*

*Lewis Research Center*

*Cleveland, Ohio 44135*

# LIQUID INFLOW TO INITIALLY EMPTY CYLINDRICAL

## TANKS IN LOW GRAVITY

by Charles M. Spuckler

Lewis Research Center

### SUMMARY

An experimental investigation was performed to determine the characteristics of liquid inflow to initially empty cylindrical tanks in a low gravity environment. The acceleration was varied so that Bond numbers based on the inlet radius varied from 0.059 to 2.80. The liquid entered the tank as a jet that grew to a maximum height and then decreased in height with respect to the bottom of the tank, with the liquid from the jet collecting in the bottom of the tank. The maximum jet heights were correlated in terms of the Weber number and the Bond number.

### INTRODUCTION

Long-term, reusable and economic space vehicles for future missions will require the resupply of their liquid systems in reduced-gravity environments. Examples are the refueling of space-vehicle propellant tanks and the resupply of regenerative life-support systems for manned spacecraft. A knowledge of the fluid behavior during the resupply (filling) of tanks under weightlessness and in reduced-gravity environments is required for systems such as these. The Lewis Research Center is presently conducting experimental programs investigating this phenomenon.

In previous studies (refs. 1 to 5), the problem of liquid inflow to both initially empty and partly full tanks under zero-gravity conditions was experimentally investigated. In these investigations it was found, depending on the inlet velocity of the liquids, that the interface was either stable (geyser formed and remained at the same height or decreased in height) or unstable (geyser continued to increase in height). In references 1 and 2 it was determined that a critical Weber number delineated the stable and unstable regions of inflow into initially empty, hemispherical-ended, cylindrical tanks. In reference 6, inflow to a spherical tank containing a spherical internal surface-tension device was

studied in a weightless environment. The only known work on inflow to tanks under low-gravity conditions is reference 7, which presents an analytical technique that predicts the transient variation in the thermodynamic properties of fluids entering a tank.

This report presents the results of an investigation to determine the characteristics of liquid inflow to cylindrical tanks in a low-gravity environment. This experimental investigation of liquid inflow to initially empty hemispherical-ended cylinders was conducted in the NASA Lewis Research Center's Zero-Gravity Facility. The acceleration was varied so that Bond numbers based on inlet radius range between 0.059 and 2.80.

## SYMBOLS

a	acceleration, $\text{cm/sec}^2$
Bo	Bond number, $ar_i^2/\beta$
d	diameter, cm
h	maximum jet height with respect to the bottom of the tank, cm
Re	Reynolds number, $Vd_i/\nu$
r	radius, cm
V	average inflow velocity, cm/sec
We	Weber number, $V^2r_i/\beta$
$\beta$	specific surface tension, $\sigma/\rho$ , $\text{cm}^3/\text{sec}^2$
$\mu$	viscosity, $\text{g}/(\text{cm})(\text{sec})$
$\nu$	kinematic viscosity, $\mu/\rho$ , $\text{cm}^2/\text{sec}$
$\rho$	density, $\text{g}/\text{cm}^3$
$\sigma$	surface tension, N/m (dynes/cm)

### Subscripts:

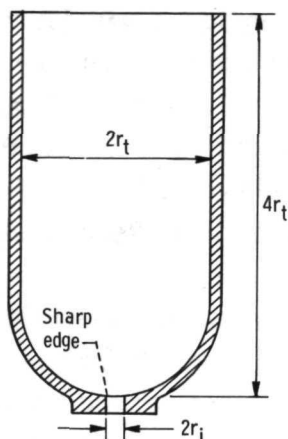
i	inlet
t	tank

## APPARATUS AND PROCEDURE

The experimental data for this study were obtained in the Zero-Gravity Facility at the Lewis Research Center. A complete description of the facility, the experiment vehicle, and their operating procedures is contained in the appendix.

The experimental tanks used in this investigation were cylindrical tanks with radii of 7.5 and 15 centimeters, with hemispherical inlet ends. The tanks and their pertinent dimensions are illustrated in figure 1. The tanks were machined from cast acrylic plastic and polished for photographic purposes.

The liquids used in this investigation were anhydrous ethanol and trichlorotrifluoroethane. Properties pertinent to the study are given in table I. The liquids had an essentially zero-degree contact angle with the acrylic plastic to duplicate the static contact angle of most liquids of interest on typical tank materials. A small amount of dye was



Tank radius, $r_t$ , cm	Inlet-line radius, $r_i$ , cm
15	1.5
15	.75
7.5	.75

Figure 1. - Experiment tanks.

TABLE I. - PROPERTIES OF TEST LIQUIDS

[Contact angle with cast acrylic plastic in air,  $0^\circ$ .]

Liquid	Surface tension at $20^\circ\text{C}$ , $\sigma$		Density at $20^\circ\text{C}$ , $\rho$ , $\text{g/cm}^3$	Viscosity at $20^\circ\text{C}$ , $\mu$ , $\text{g/cm-sec}$	Specific surface tension, $\beta$ , $\text{cm}^3/\text{sec}^2$
	N/m	dynes/cm			
Anhydrous ethanol	$22.3 \times 10^{-3}$	22.3	0.79	$1.2 \times 10^{-2}$	28.3
Trichlorotrifluoroethane	$18.6 \times 10^{-3}$	18.6	1.58	$.7 \times 10^{-2}$	11.8

added to the liquid to improve photographic quality. Previous studies have determined that the dye has no measurable effect on the fluid properties.

## RESULTS AND DISCUSSION

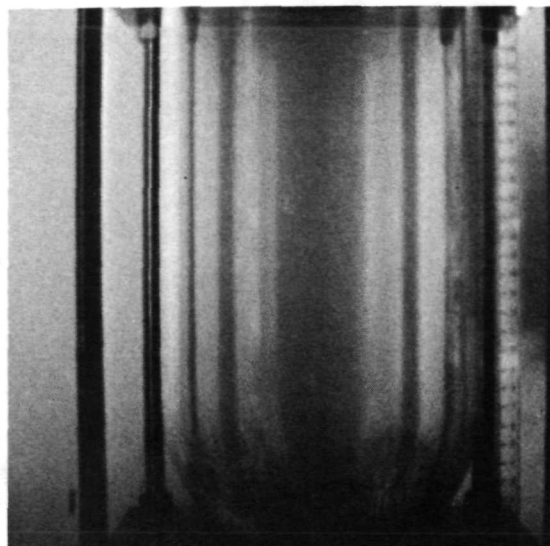
### Description of Inflow Phenomena

In the studies of liquid inflow to tanks in a zero-gravity environment conducted in references 1 and 2, the incoming liquid jet was determined to be either stable or unstable. The stable jet was defined as one which grew to some height with respect to the liquid vapor interface and either remained at that height or decreased in height with respect to the lowest point on the interface. The unstable jet was one which continued to grow or which broke up into droplets or globules. Furthermore, the stability of the liquid vapor interface was correlated by a Weber number based on inlet line radius and inlet velocity.

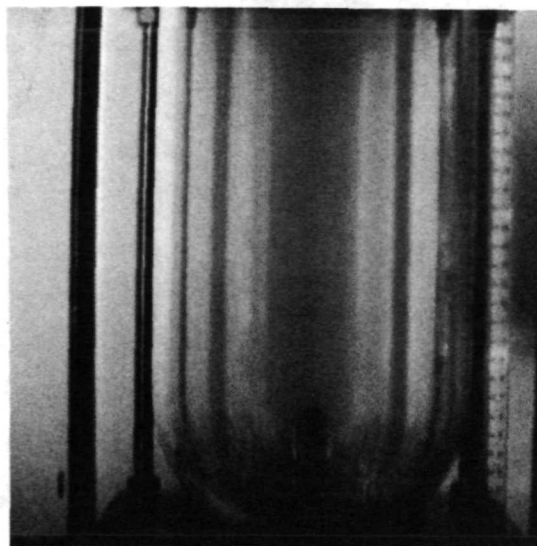
The present experimental program was conducted in a low-gravity environment over a range of Bond numbers from 0.059 to 2.80, based on inlet-line radius. Weber numbers, based on inlet conditions as in references 1 and 2, ranged from 3.44 to 27.0. No instabilities such as those previously described were observed. In all cases, the liquid flowing into the tank entered as a jet which grew to a maximum height with respect to the bottom of the tank. When the jet was near or at its maximum height, the radius of the jet increased. After reaching a maximum height and while increasing in radius, the jet decreased in height with respect to the bottom of the tank, with the liquid from the jet collecting in the bottom of the tank.

Photographs showing liquid inflow phenomena for laminar ( $Re < 2000$ ) and turbulent ( $Re > 4000$ ) flows are presented in figure 2. Figure 2(a) presents a photographic sequence of laminar liquid inflow into a 7.5-centimeter-radius tank with a 0.75-centimeter-radius inlet. The liquid was ethanol, the flow rate was 17.0 centimeters per second, and the Bond number was 0.293. These photographs show that when the liquid entered the tank, the radius of the jet became slightly larger than the inlet radius (time 0.54 sec). The jet then narrowed as it continued to grow (time 1.08 sec), and reached a maximum height (time 2.30 sec). The jet then started to increase in radius and decrease in height with respect to the bottom of the tank, with the liquid from the jet collecting in the bottom of the tank (time 3.28 sec).

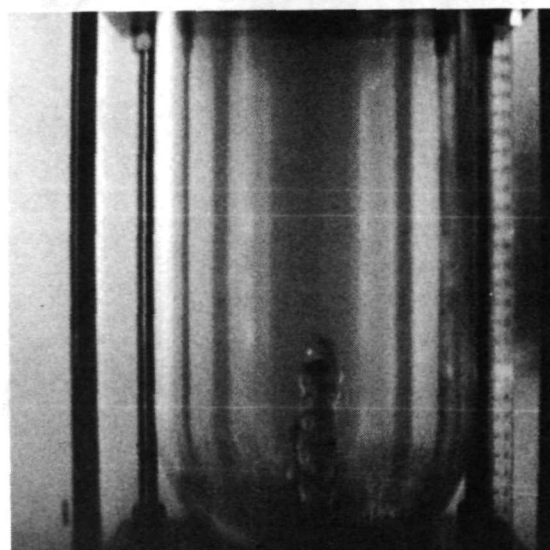
Figure 2(b) presents a photographic sequence of turbulent liquid inflow into a 15-centimeter-radius tank with a 1.5-centimeter-radius inlet. The test liquid was trichlorotrifluoroethane, the flow rate was 12.0 centimeters per second, and the Bond number was 2.43. The liquid enters the tank (time 0.42 sec), and as the inflow pro-



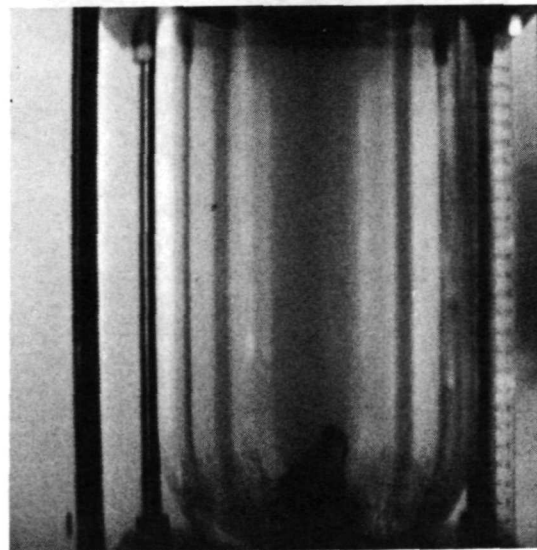
Time, 0.54 sec



Time, 1.08 sec



Time, 2.30 sec



Time, 3.28 sec

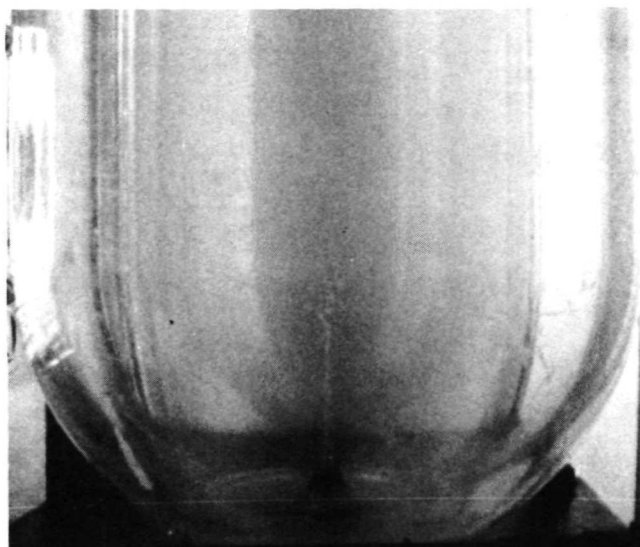
(a) Laminar flow regime. Tank radius, 7.5 cm; inlet radius, 0.75 cm; test liquid, ethanol; flow rate, 17.0 cm/sec; Bond number, 0.293.

Figure 2. - Liquid inflow phenomena in low-gravity.





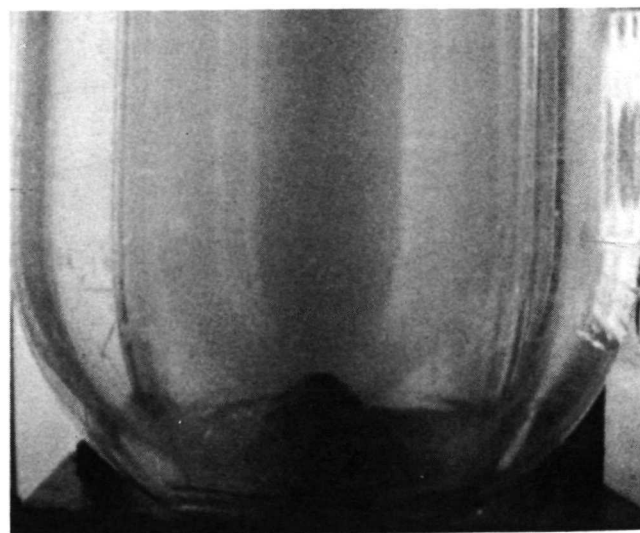
Time, 0.42 sec



Time, 2.30 sec



Time, 3.30 sec



Time, 4.55 sec

(b) Turbulent flow regime. Tank radius, 15 cm; inlet radius, 1.5 cm; test liquid, trichlorotrifluoroethane; flow rate, 12.0 cm/sec; Bond number, 2.43.

Figure 2. Concluded.

ceeds, the jet radius increases and becomes slightly larger than the inlet radius (time 2.30 sec). The jet then narrows slightly and continues to grow until it reaches a maximum height, with some liquid collecting in the bottom of the tank (time 3.30 sec). The jet then increased in radius and decreased in height, with the liquid from the jet collecting in the bottom of the tank (time 4.55 sec).

## Inflow Parameters in Low Gravity

The three main forces that determine the jet height in a low-gravity environment are the inertia force, the gravitational force, and the surface-tension force. These forces lead to the inlet radius  $r_i$ , inlet velocity  $V$ , density  $\rho$ , surface tension  $\sigma$ , acceleration  $a$ , and the jet height  $h$  as the important parameters in this study. A dimensional analysis using the Buckingham theorem yields two dimensionless groups. One group contains the Froude number ( $V^2/r_i a$ ), the ratio  $h/r_i$ , and the Bond number. The other group contains the Weber number ( $V^2 r_i / \beta$ ), the ratio  $h/r_i$ , and the Bond number. The Froude number is the ratio of inertial to acceleration forces, and the Weber number is the ratio of inertial to surface-tension forces. The grouping containing the Weber number was found to normalize the data, while the other dimensionless group did not. This implies that the surface-tension force was the dominant force over the range of accelerations (0.003 to 0.015 g) used. The nondimensional parameters used and results obtained in the study are presented in table II.

## Effect of Jet Reynolds Number

The range of Reynolds number ( $1415 \leq Re \leq 9870$ ) used in this study covered the laminar, transition, and turbulent flow regimes. The laminar- and transition-flow-regime ( $Re < 4000$ ) data are presented in figure 3. No discernible differences could be ascertained for these two flow regimes. The turbulent-flow-regime ( $4000 < Re < 9900$ ) data are presented in figure 4. In each figure, a line faired through the data shows that the nondimensional height parameter  $We/(h/r_i)$  increases with the Bond number. The dependence of the maximum jet height  $h$  on the Bond number can be determined from these figures. For a given Weber number, the maximum jet height decreases with increasing Bond number. It is reasonable to assume that the maximum jet height will occur when there is no liquid in the bottom of the tank. When there is liquid in the bottom of the tank, the jet must pass through it, transferring some of its axial momentum to the bulk liquid. This will cause the jet to spread so that the inertial force will tend to equal the gravitational and surface-tension forces at a lower jet height; therefore,



TABLE II. - SUMMARY OF LOW-GRAVITY DATA

Tank radius, $r_t$ , cm	Inlet radius, $r_i$ , cm	Test liquid	Bond number, $Bo$	Weber number, $We$	Ratio of maximum jet height to inlet radius, $h/r_i$	Flow regime
7.5	0.75	Ethanol	0.059	5.31	29.8	Laminar
			.137	6.67	25.1	Laminar
			.214	12.3	30.1	Transition
			.293	7.65	14.9	Laminar
		TCTFE <sup>a</sup>	0.140	3.44	7.13	Transition
			.327	4.58	7.87	↓
			.327	8.98	14.2	
			.514	4.58	7.08	
			.514	16.0	15.0	Turbulent
			.701	6.59	6.91	Transition
			.701	12.7	11.0	Turbulent
			.701	18.3	15.3	Turbulent
15	0.75	Ethanol	0.098	5.31	25.1	Laminar
			.176	12.3	39.9	Transition
			.234	13.6	35.8	Transition
			.293	13.6	29.2	Transition
		TCTFE <sup>a</sup>	0.140	3.44	9.09	Transition
			.327	8.98	13.6	Transition
			.514	4.58	6.95	Transition
			.701	12.7	11.1	Turbulent
15	1.5	Ethanol	0.390	7.06	9.15	Transition
			.546	8.04	8.30	↓
			.858	9.59	7.99	
			1.17	10.2	7.15	
		TCTFE <sup>a</sup>	0.561	4.49	3.37	Turbulent
			.934	5.69	3.65	↓
			.934	10.4	7.12	
			1.31	10.4	6.33	
			1.31	13.9	6.74	
			1.87	11.4	5.87	
			1.87	18.6	8.26	
			2.06	23.0	7.74	
			2.43	12.5	5.79	
			2.43	18.4	6.80	
			2.43	26.5	8.54	
			2.80	16.3	5.08	
			2.80	27.0	8.27	↓

<sup>a</sup>Trichlorotrifluoroethane.

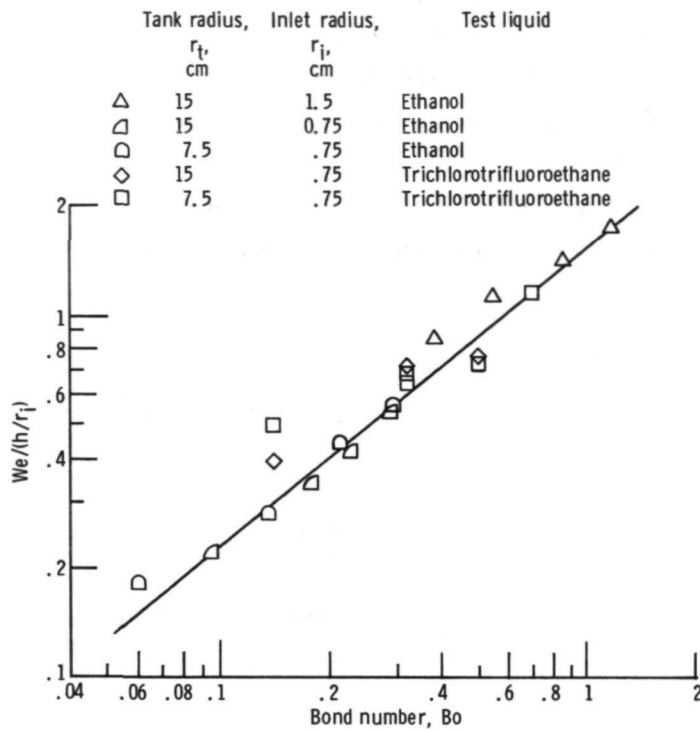


Figure 3. - Dependence of jet height on system parameters with liquid flow in the laminar and transition regimes. Reynolds number,  $< 4000$ .

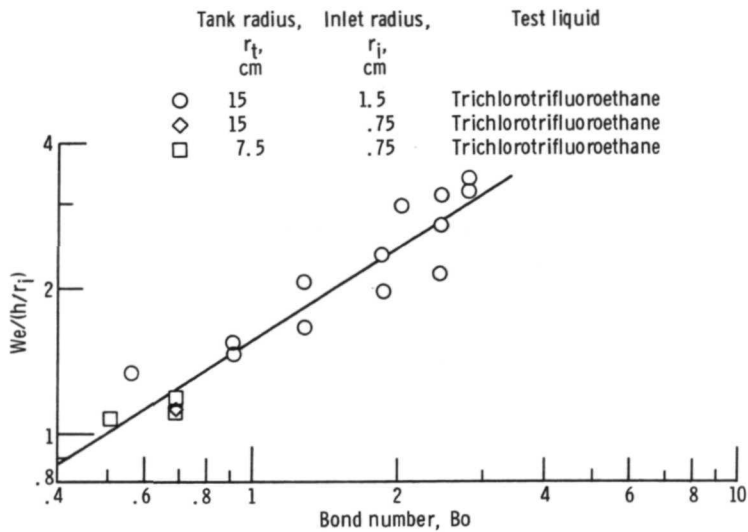


Figure 4. - Dependence of jet height on system parameters with liquid flow in the turbulent flow regime. Reynolds number range, 4000 to 9900.

the jet height should decrease as the liquid level in the tank increases. As mentioned earlier, the jet height is referenced to the bottom of the tank.

The laminar-, transition-, and turbulent-inflow data are compared in figure 5. This figure shows that the rate of increase of the nondimensional height parameter  $We/(h/r_i)$  with Bond number is greater for the laminar and transition flow regimes than for the turbulent-flow regimes. The data for the laminar- and transition-flow regimes overlap the data for the turbulent-flow regime over a range of Bond numbers from 0.514 to 1.17. Over this range of Bond numbers, the nondimensional height parameter

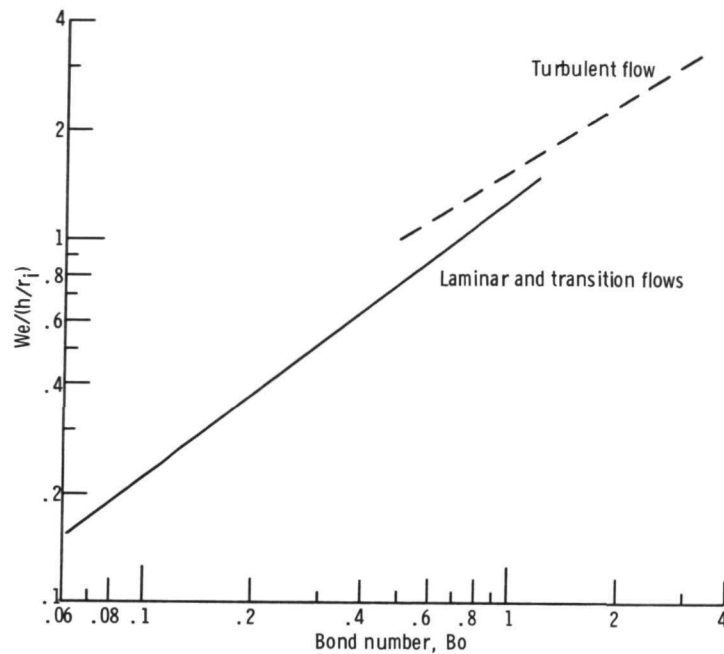


Figure 5. - Dependence of jet height on system parameters and velocity profiles.

$We/(h/r_i)$  has a greater value for turbulent flow than for laminar and transitions flows. Thus, to attain the same jet height at a given Bond number, a higher inflow velocity is required when the flow is turbulent. This is due to the fact that the difference between the maximum and average jet velocities is less for turbulent flow than for laminar or transition flow.

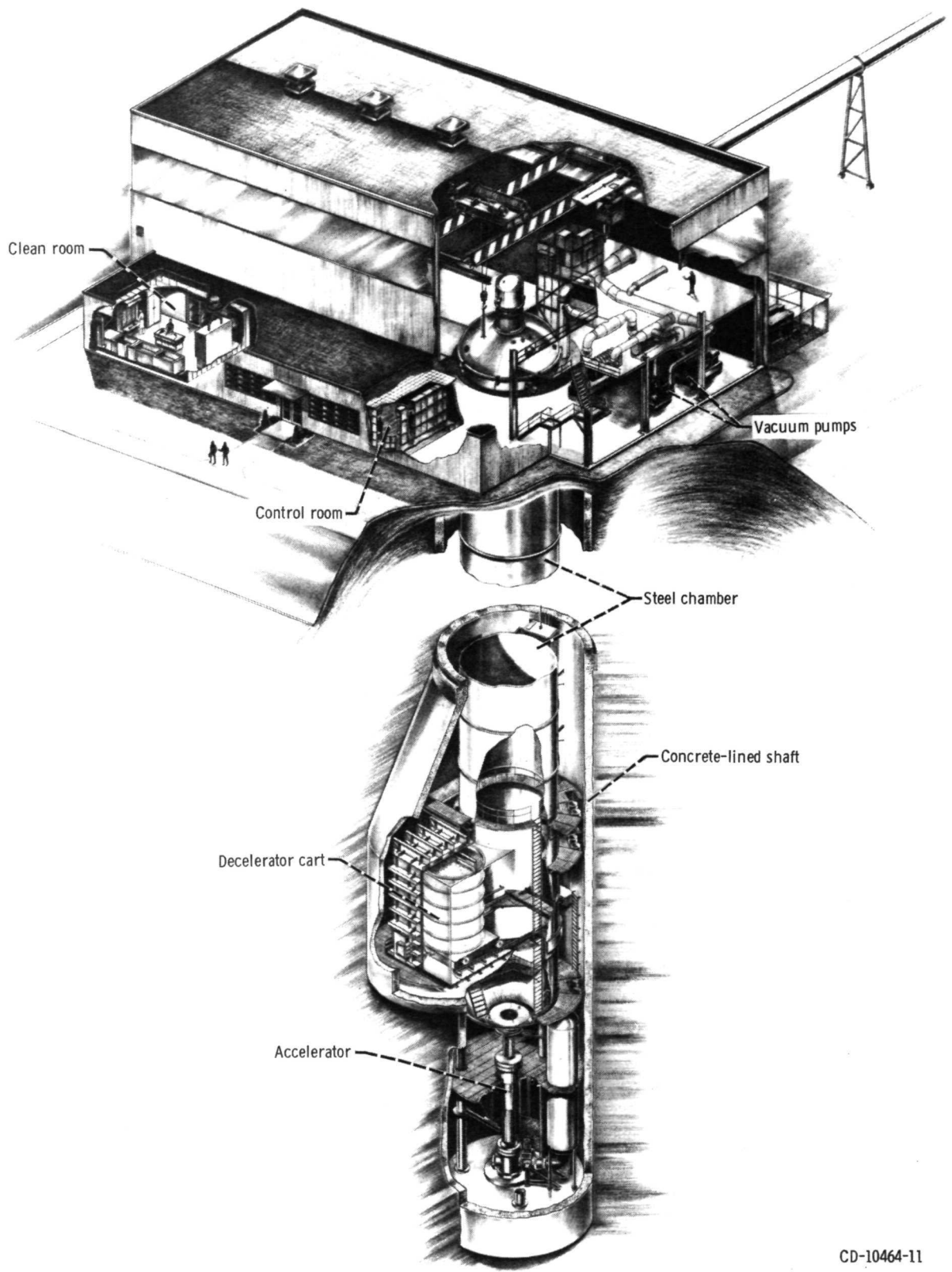
## SUMMARY OF RESULTS

An experimental investigation was performed to determine the characteristics of liquid inflow to initially empty cylindrical tanks in a low gravity environment. Cylindrical

tanks having hemispherical inlet ends, radii of 7.5 and 15 centimeters, and inlet radii of 0.75 and 1.5 centimeters were used. The test liquid used in the study were anhydrous ethanol and trichlorotrifluoroethane. The acceleration was varied so that Bond numbers based on inlet radius ranged from 0.059 to 2.80. The following results were obtained:

1. The inflow jet grew to a maximum height and then decreased in height, with liquid collecting in the bottom of the tank. No instability was observed over the range of Weber numbers (3.44 to 27.0) used in the tests.
2. A nondimensional jet height parameter  $We/(h/r_i)$ , where  $We$  is the Weber number,  $h$  is the maximum jet height, and  $r_i$  is the radius of the inlet, was correlated with Bond number both for the laminar and transition flow regimes and for the turbulent flow regime.
3. The rate of increase of  $We/(h/r_i)$  with Bond number was greater for the laminar and transition flow regimes than for the turbulent flow regime.
4. Where the correlations overlap, the nondimensional jet height parameter  $We/(h/r_i)$  is greater for the turbulent flow regime.

Lewis Research Center,  
National Aeronautics and Space Administration,  
Cleveland, Ohio, June 1, 1972,  
113-31.



CD-10464-11

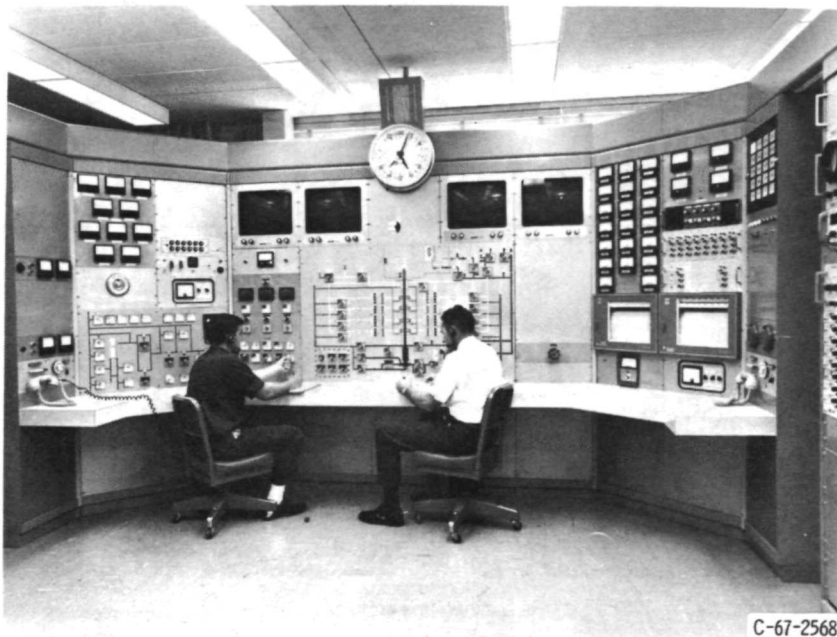
Figure 6. - Zero-Gravity Facility.

## APPENDIX - APPARATUS AND PROCEDURE

### Test Facility

The experiment data for this study were obtained in the Zero-Gravity Facility at the Lewis Research Center. A schematic diagram of this facility is shown in figure 6. The facility consists of a concrete-lined, 8.5-meter-diameter (28-ft-diam) shaft that extends 155 meters (510 ft) below ground level. A steel vacuum chamber, 6.1 meters (20 ft) in diameter and 143 meters (470 ft) high, is contained within the concrete shaft. The pressure in this vacuum chamber is reduced to 13.3 newtons per square meter ( $1.3 \times 10^{-4}$  atm) by utilizing the Center's wind-tunnel exhaust system and an exhaustor system located in the facility.

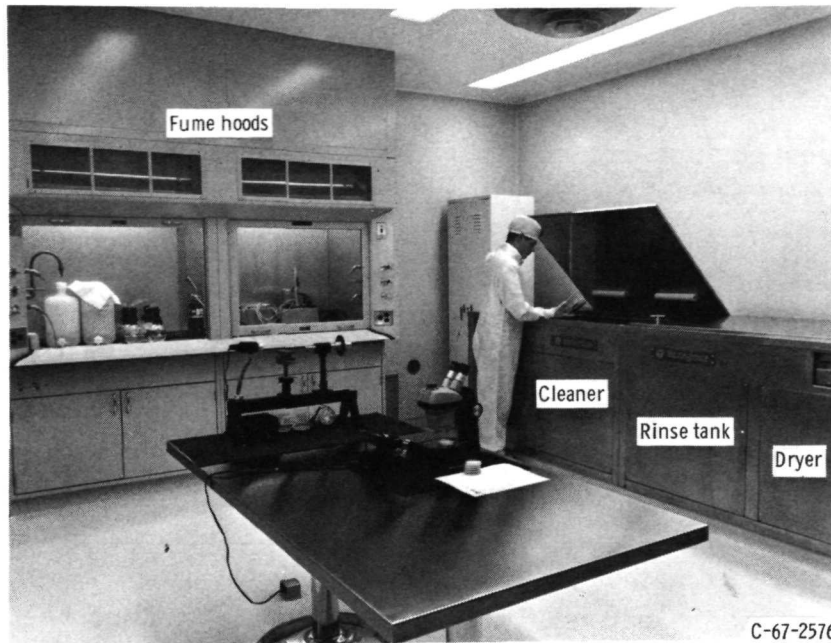
The ground-level service building has, as its major elements, a shop area, a control room, and a clean room. Assembly, servicing, and balancing of the experiment vehicle are accomplished in the shop area. Tests are conducted from the control room (fig. 7), which contains the exhaustor control system, the experiment vehicle predrop checkout and control system, and the data retrieval system. Those components of the experiment which are in contact with the test fluid are prepared in the facility's class 10 000 clean room. The major elements of the clean room are an ultrasonic cleaning system (fig. 8(a)) and a class 100 laminar-flow work station (fig. 8(b)) for preparing those experiments that require more than normal cleanliness.



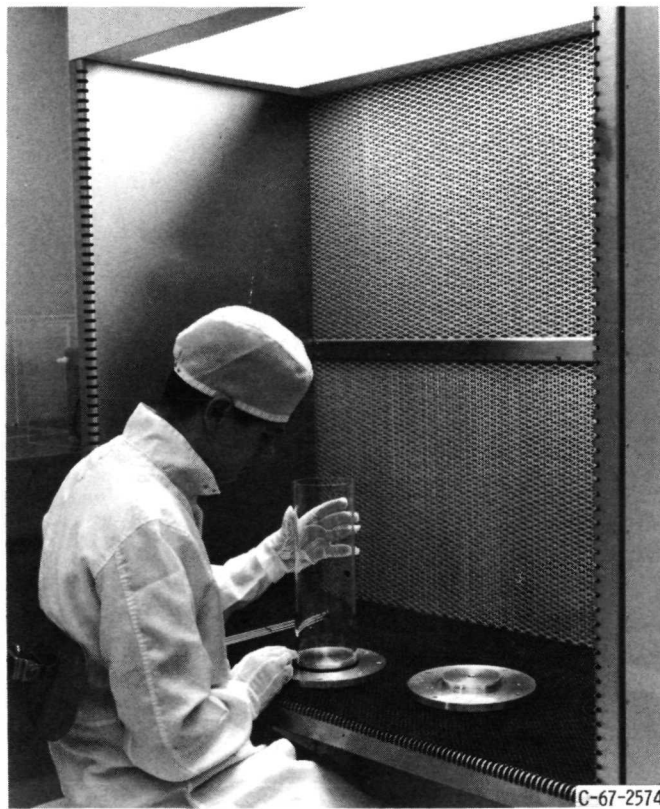
C-67-2568

Figure 7. - Control room.





(a) Ultrasonic cleaning system.



(b) Laminar-flow work station.

Figure 8. - Clean room.

Mode of operation. - The Zero-Gravity Facility has two modes of operation. One is to allow the experiment vehicle to fall freely from the top of the vacuum chamber, which results in nominally 5 seconds of free-fall time. The second mode is to project the experiment vehicle upwards from the bottom of the vacuum chamber by a high-pressure pneumatic accelerator located on the vertical axis of the chamber. The total up-and-down trajectory of the experiment vehicle results in nominally 10 seconds of free-fall time. The 5-second mode of operation was used for this experimental study.

In either mode of operation, the experiment vehicle falls freely; that is, no guide wires, electrical lines, etc., are connected to the vehicle. Therefore, the only force (aside from gravity) acting on the freely falling experiment vehicle is due to residual air drag. This results in an equivalent gravitational acceleration acting on the experiment which is estimated to be of the order of  $10^{-5}$  g maximum.

Recovery system. - After the experiment vehicle has traversed the total length of the vacuum chamber, it is decelerated in a 3.6-meter- (12-ft-) diameter, 6.1-meter- (20-ft-) deep container which is located on the vertical axis of the chamber and filled with small pellets of expanded polystyrene. The deceleration rate (averaging 32 g's) is controlled by the flow of pellets through the area between the experiment vehicle and the wall of the deceleration container. This deceleration container is mounted on a cart which can be retracted prior to utilizing the 10-second mode of operation. In this mode of operation, the cart is deployed after the experiment vehicle is projected upward by the pneumatic accelerator. The deceleration container mounted on the cart is shown in the photograph of figure 9.

## Experiment Vehicle

The experiment vehicle used to obtain the data for this study is shown in figure 10. The overall vehicle height (exclusive of the support shaft) is 3.0 meters (9.85 ft), and the largest diameter is 1.06 meters (3.5 ft). The vehicle consists of a telemetry section contained in the aft fairing, a thrust system contained in the conical base and an experiment section housed in the cylindrical midsection.

Telemetry system. - The on-board telemetry system which is used to record pressure data is a standard Inter-Range Instrumentation Group (IRIG) FM/FM 2200-megahertz telemeter. It is used during a test drop to record up to 18 channels of continuous data. The system has a frequency range up to 2100 hertz. The telemetered data are recorded on two high-response recording oscillographs located in the control room.

Thrust system. - The self contained cold-gas thrust system housed in the conical base of the experiment produced thrust values ranging from 13 to 130 newtons (3 to 30 lb) for time durations longer than 5 seconds. Steady-state response time was better than

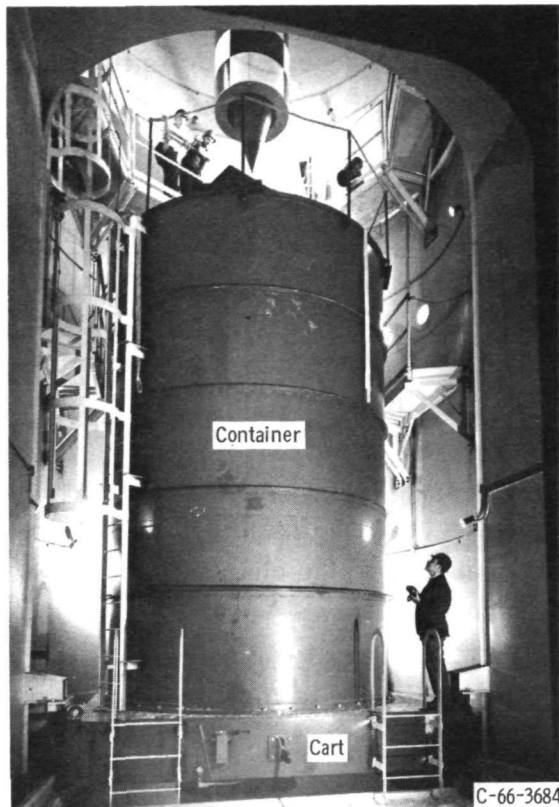


Figure 9. - Deceleration system.

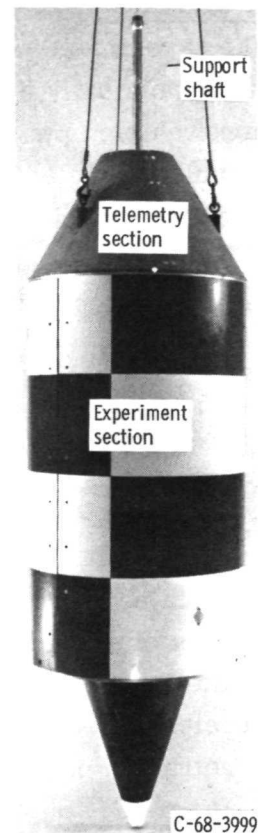


Figure 10. - Experiment vehicle.

50 milliseconds. The thrust system was calibrated in the facility's main chamber at vacuum levels corresponding to test-drop conditions. The thrust curves were related to the pressure recorded at the inlet of the thrust nozzle. The magnitude of the thrust was set by changing the nozzle configuration, the regulator pressure, or the weight of the vehicle.

Experiment. - The experiment section consists of the test tank, the pressurization the flow-control system, and the necessary photographic equipment. The details of the experiment section are shown in figure 11. The experiment tank is mounted in such a way that the motion of the liquid-vapor interface during inflow can be recorded by means of a high-speed motion-picture camera. Both a sweep-hand clock having an accuracy of  $\pm 0.005$  second and a centimeter scale are positioned in the field of view of the camera. In order to provide adequate lighting for the photography, the experiment is lighted with an array of spotlights. Differential pressure is maintained by the pressure regulator during the inflow process and is continuously recorded by telemetry.

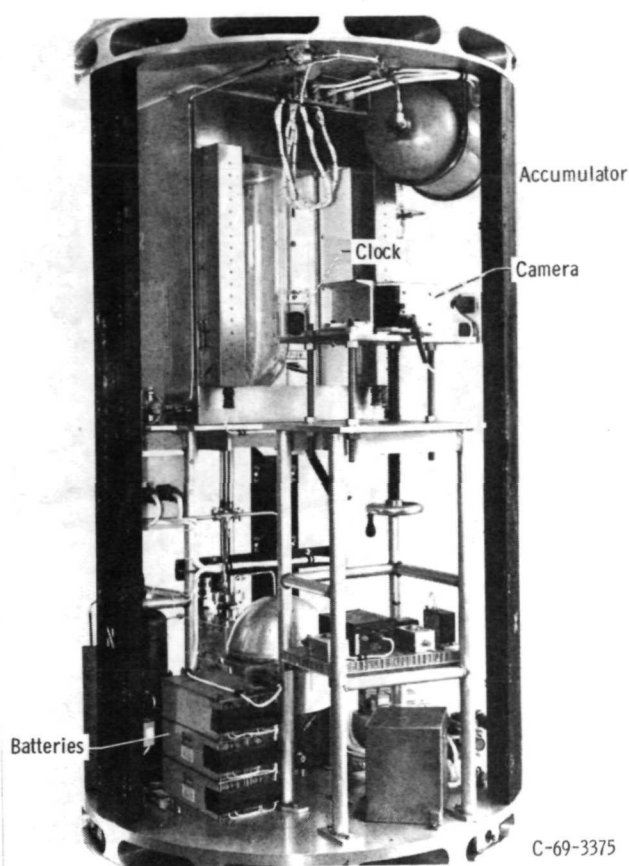
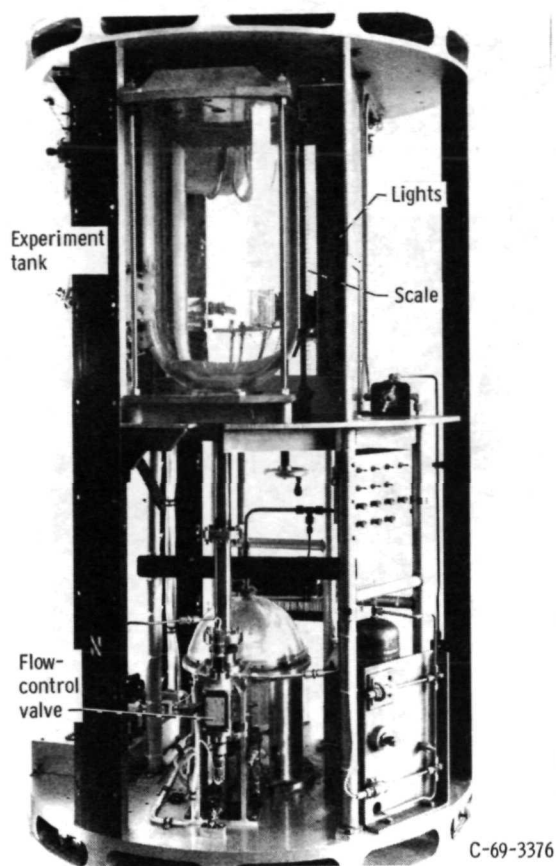


Figure 11. - Experiment section details.

## Test Procedure

Prior to each test, the tank was thoroughly washed, ultrasonically cleaned, dried in a warm-air dryer, and assembled in the clean room. The clean tank was then installed in the experiment vehicle.

The liquid velocity was set for each test drop by a normal gravity calibration check. The desired velocity was obtained by regulating the pressure across an orifice and then opening a fast-acting solenoid valve to initiate flow into the experiment tank. A calibration curve which gave flow rate against pressure for a given orifice size was used to determine approximate settings, and these were verified for each drop by measuring the volume of liquid pumped into the tank in a given period of time. Effects of static head were negligible, and inflow to the experiment was started at the initiation of weightlessness. The thrust was set for each test by changing either the nozzle configuration or the regulator pressure.

The vehicle was positioned at the top of the vacuum chamber as shown in figure 12.

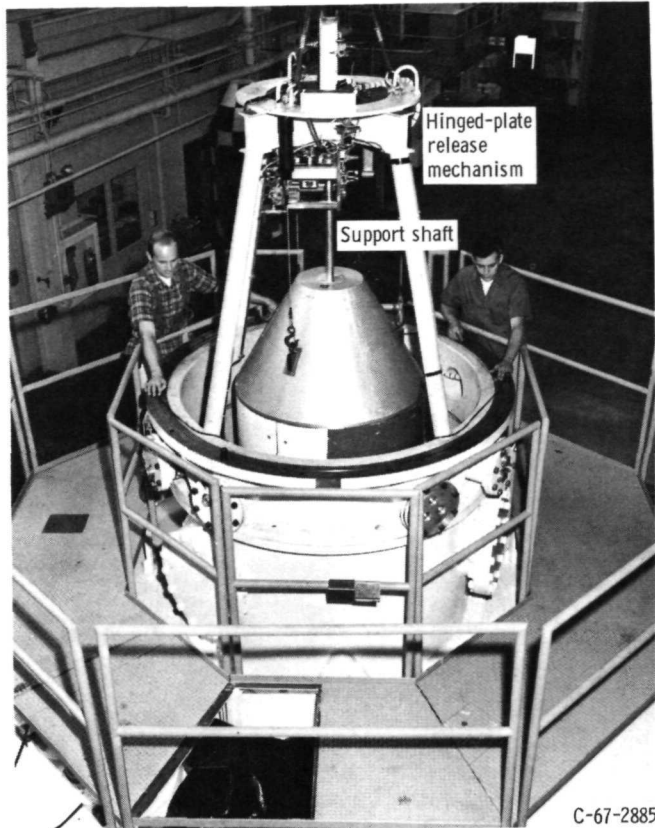


Figure 12. - Typical vehicle positioning prior to release.

It was suspended by the support shaft on a hinged-plate release mechanism. During vacuum-chamber pumpdown and prior to release, monitoring of experiment-vehicle systems was accomplished through an umbilical cable attached to the top of the support shaft. Electrical power was supplied from ground equipment. The system was then switched to internal power a few minutes before release. The thruster was activated 0.2 second before release to allow the thrust to reach steady-state conditions. The vehicle was released by pneumatically shearing a bolt that was holding the hinged plate in the closed position. No measurable disturbances were imparted to the experiment vehicle by this release procedure.

The total free-fall test time obtained in this mode of operation is 5.16 seconds. During the test drop, the vehicle's trajectory and deceleration were monitored on closed-circuit television. Following the test drop, the vacuum chamber was vented to the atmosphere, and the experiment was returned to ground level (see fig. 13).



Figure 13. - Experiment vehicle being returned to ground level.



## REFERENCES

1. Symons, Eugene P.; Nussle, Ralph C.; and Abdalla, Kaleel L.: Liquid Inflow to Initially Empty, Hemispherical Ended Cylinders During Weightlessness. NASA TN D-4628, 1968.
2. Symons, Eugene P.: Interface Stability During Liquid Inflow to Initially Empty Hemispherical Ended Cylinders in Weightlessness. NASA TM X-2003, 1970.
3. Symons, Eugene P.; and Nussle, Ralph C.: Observations of Interface Behavior During Inflow to an Elliptical Ended Cylinder in Weightlessness. NASA TM X-1719, 1969.
4. Symons, Eugene P.: Liquid Inflow to Partly Full, Hemispherical-Ended Cylinders During Weightlessness. NASA TM X-1934, 1969.
5. Symons, Eugene P.; and Staskus, John V.: Interface Stability During Liquid Inflow to Partially Full, Hemispherical Ended Cylinders During Weightlessness. NASA TM X-2348, 1971.
6. Andracchio, Charles R.; and Abdalla, Kaleel L.: An Experimental Study of Liquid Flow into a Baffled Spherical Tank During Weightlessness. NASA TM X-1526, 1968.
7. Vernon, R. M.; and Brogan, J. J.: A Study of Cryogenic Container Thermodynamics During Propellant Transfer. Vol. IV: Tank Fill Thermodynamic Analysis. Rep. K-14-67-3, vol. 4, Lockheed Missiles and Space Co. (NASA CR-90349), Nov. 30, 1967.



POSTMASTER: If Undeliverable (Section 158  
Postal Manual) Do Not Return

*"The aeronautical and space activities of the United States shall be conducted so as to contribute . . . to the expansion of human knowledge of phenomena in the atmosphere and space. The Administration shall provide for the widest practicable and appropriate dissemination of information concerning its activities and the results thereof."*

—NATIONAL AERONAUTICS AND SPACE ACT OF 1958

## NASA SCIENTIFIC AND TECHNICAL PUBLICATIONS

**TECHNICAL REPORTS:** Scientific and technical information considered important, complete, and a lasting contribution to existing knowledge.

**TECHNICAL NOTES:** Information less broad in scope but nevertheless of importance as a contribution to existing knowledge.

**TECHNICAL MEMORANDUMS:** Information receiving limited distribution because of preliminary data, security classification, or other reasons.

**CONTRACTOR REPORTS:** Scientific and technical information generated under a NASA contract or grant and considered an important contribution to existing knowledge.

**TECHNICAL TRANSLATIONS:** Information published in a foreign language considered to merit NASA distribution in English.

**SPECIAL PUBLICATIONS:** Information derived from or of value to NASA activities. Publications include conference proceedings, monographs, data compilations, handbooks, sourcebooks, and special bibliographies.

**TECHNOLOGY UTILIZATION PUBLICATIONS:** Information on technology used by NASA that may be of particular interest in commercial and other non-aerospace applications. Publications include Tech Briefs, Technology Utilization Reports and Technology Surveys.

*Details on the availability of these publications may be obtained from:*

**SCIENTIFIC AND TECHNICAL INFORMATION OFFICE**

**NATIONAL AERONAUTICS AND SPACE ADMINISTRATION**

Washington, D.C. 20546